Genomics 92 (2008) 26–32

Contents lists available at ScienceDirect

Genomics

journal homepage: www.elsevier.com/locate/ygeno

Differential transcriptional modulation of biological processes in adipocyte triglyceride lipase and hormone-sensitive lipase-deficient mice

Montserrat Pinent [a,1], Hubert Hackl [a,1], Thomas Rainer Burkard [a,b], Andreas Prokesch [a], Christine Papak [a], Marcel Scheideler [a], Günter Hämmerle [c], Rudolf Zechner [c], Zlatko Trajanoski [a,*], Juliane Gertrude Strauss [a]

[a] Institute for Genomics and Bioinformatics, Graz University of Technology, 8010 Graz, Austria
[b] Research Institute of Molecular Pathology, Vienna, Austria
[c] Institute for Molecular Biosciences, Karl-Franzens University Graz, Graz, Austria

ARTICLE INFO

Article history:
Received 7 January 2008
Accepted 7 March 2008

Keywords:
Expression profiling
Microarrays
Lipid metabolism

ABSTRACT

Adipocyte triglyceride lipase (ATGL) and hormone-sensitive lipase (HSL) are intracellular lipases that mobilize triglycerides, the main energy source in mammals. Deletion of genes encoding ATGL (Pnpla2) or HSL (Lipe) in mice results in striking phenotypic differences, suggesting distinct roles for these lipases. The goal of the present study was to identify the biological processes that are modulated in the metabolic tissues of ATGL- and HSL-deficient mice. DNA microarrays were employed to provide full genome coverage concerning the types of genes that are differentially expressed in wild-type and mutant mice. For both mouse models, transcript signatures were identified in white adipose tissue, brown adipose tissue (BAT), skeletal muscle (SM), cardiac muscle (CM), and liver. Genetic ablation of ATGL and HSL alters the transcript levels of a large number of genes in metabolic tissues. The genes affected in the two models are, however, largely different ones. Indeed, only one biological process was modulated in the same way in both mouse models, namely the down-regulation of fatty acid metabolism in BAT. The most pronounced modulation of biological processes was observed in $ATGL^{-/-}$ CM, in which a concerted down-regulation of transcripts associated with oxidative pathways was observed. In $HSL^{-/-}$ mice, in contrast, the most marked changes were seen in SM, namely, alterations in transcript levels reflecting a change of energy source from lipid to carbohydrate. The transcript signatures also provided novel insights into the metabolic derangements that are characteristic of $ATGL^{-/-}$ mice. Our findings suggest that ATGL and HSL differentially modulate biological processes in metabolic tissues. We hypothesize that the intermediary metabolites of the lipolytic pathways are signaling molecules and activators of a wide range of biochemical and cellular processes in mammals.

Triglycerides (TGs), stored in adipose tissue, are the main energy source of mammals. TG stores are constantly turned over and tightly regulated according to the needs of the organism. Indicative of this, imbalances in TG metabolism are linked to metabolic disorders such as obesity and diabetes [1,2]. TGs are hydrolyzed (mobilized) by lipases in a regulated manner to release fatty acids. Until recently, hormone sensitive lipase (HSL) was considered to be the most important lipase for the hydrolysis of intracellular TGs and diglycerides (DGs) [3]. HSL-deficient mice are, however, nonobese [4–6] and are resistant to diet-induced obesity [7], suggesting that another lipase catalyzes the initial step in TG hydrolysis. This enzyme, adipocyte triglyceride lipase (ATGL), also known as desnutrin and calcium-independent phospholipase A2ζ [8,9], was recently discovered [10] and shown to catalyze the initial step in TG hydrolysis. HSL catalyzes the rate-limiting step in the catabolism of DGs. ATGL is expressed mainly in adipose tissue and to a lesser extent in testis, cardiac muscle, and skeletal muscle [9,10]. In vitro experiments have demonstrated that the role played by ATGL in lipid storage and degradation in adipose tissue is also important in cell types other than adipocytes [11].

The important role of ATGL in the mobilization of fat stores in vivo was recently demonstrated using an ATGL-deficient mouse model [12]. Unlike $HSL^{-/-}$ mice, $ATGL^{-/-}$ mice have increased TG deposition in several tissues and exhibit mild obesity caused by enlarged adipose lipid droplets. Notably, severe fat accumulation in cardiac muscle in these mice leads to cardiac insufficiency and premature death. $ATGL^{-/-}$ mice furthermore exhibit increased sensitivity to low temperatures due to defects in thermogenesis. Other notable features of ATGL-deficient mice are increased glucose tolerance, increased insulin sensitivity, and increased respiratory quotient during fasting, suggesting the use of glucose as metabolic fuel [12].

The striking phenotypic differences between these lipase-deficient mouse strains with defects at adjacent steps in the same metabolic pathway vividly demonstrate the highly complex and unpredictable

* Corresponding author. Fax: +43 316 873 5340.
E-mail address: zlatko.trajanoski@tugraz.at (Z. Trajanoski).
[1] These authors contributed equally to this work.

0888-7543/$ – see front matter © 2008 Elsevier Inc. All rights reserved.
doi:10.1016/j.ygeno.2008.03.010

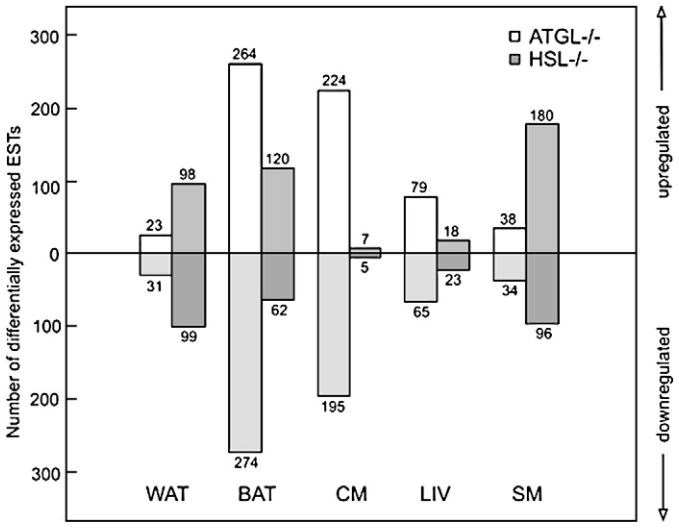

Fig. 1. Number of differentially expressed ESTs in each analyzed tissue for each mouse model, ATGL$^{-/-}$ and HSL$^{-/-}$, based on the *z* ratio.

properties of metabolic networks that comprise hundreds of interconnected biochemical reactions. Because of this interconnectivity the modification of the activity of only a single enzyme can have profound effects on the whole organism. The goal of our study was to identify the biological processes that are modulated in metabolic tissues of ATGL- and HSL-deficient mice. To avoid a priori assumptions concerning the affected processes we used whole-genome DNA microarrays for the generation of transcript signatures for white adipose tissue (WAT), brown adipose tissue (BAT), skeletal muscle (SM), cardiac muscle (CM), and liver (LIV) for each mouse model. Our findings show that genetic ablation of intracellular lipases alters the levels of transcripts for a large number of genes. Notably, the genes that are modulated in the two models are largely different ones, despite the fact that the two lipases catalyze adjacent steps in TG catabolism. Only one biological process was altered in both models in the same way, namely the down-regulation of fatty acid β-oxidation in BAT. In ATGL-deficient mice, oxidative pathways were coordinately down-regulated in CM. The largest number of deregulated genes in HSL-deficient mice was found in the SM, in which we detected changes in transcript levels consistent with a switch from lipid to carbohydrate metabolism. Finally, the changes in transcript levels and predicted changes in biological processes in the tissues of both mouse models were consistent with and to some extent accounted for the respective model phenotypes.

Results

Distinct transcript signatures in metabolic tissues of ATGL$^{-/-}$ and HSL$^{-/-}$ mice

Microarray analysis showed that a total of 628 ESTs were up- and 599 ESTs were down-regulated in ATGL$^{-/-}$ mice. The number of ESTs deregulated in HSL$^{-/-}$ mice was lower (323 ESTs up- and 285 down-regulated) (Fig. 1). The distribution of differentially expressed genes among tissues also differed between the two models. The expression levels of differentially expressed ESTs ($z>1.5$, $p<0.05$) can be viewed in Supplementary File 1. Most differentially expressed genes in ATGL$^{-/-}$ mice were found in BAT (538), followed by CM (419), and liver (144). Of these genes, only 79, 16, and 9 ESTs were also deregulated, respectively, in BAT, CM, and liver of HSL$^{-/-}$ mice (Fig. 2). In contrast, in HSL$^{-/-}$ mice the majority of differentially expressed genes were observed in SM (276), WAT (197), and BAT (182). 47, 35, and 79 ESTs that were differentially expressed in HSL$^{-/-}$ mice (in SM, WAT, and BAT, respectively) were also deregulated in ATGL$^{-/-}$ mice (Fig. 2). Additionally, the genes that were deregulated in ATGL$^{-/-}$ SM were more similar to those deregulated in HSL$^{-/-}$ BAT than in HSL$^{-/-}$ SM (Fig. 2). Interestingly, there was no relationship between the transcript signatures and the levels of expression of HSL and ATGL in the metabolic tissues (see Supplementary File 2 for the ratio of the expression levels of ATGL and HSL).

Genes differentially expressed in each mouse model were classified according to Gene Ontology (GO) [13] (see Supplementary File 3). Since ATGL and HSL are enzymes from the same metabolic pathway, similar modulation of biological pathways was expected. Significantly overrepresented GO terms (category "biological process") for up- and down-regulated genes in all ATGL$^{-/-}$ and HSL$^{-/-}$ tissues that were analyzed are shown in Fig. 3. Strikingly, only one biological process, i.e., fatty acid metabolism, was altered in the same manner in both models. In both cases it was down-regulated in BAT (Fig. 3). Lipid metabolism in BAT was modulated in both models, although in opposite directions (up-regulation in ATGL$^{-/-}$ mice and down-regulation in HSL$^{-/-}$ mice). Overall, in ATGL$^{-/-}$ mice the highest of the modulated biological processes in an individual metabolic tissue were detected in CM. In contrast, in HSL$^{-/-}$ mice, most modulated processes were found in BAT. With respect to the number of modulated processes, the tissue that was least affected was WAT.

Concerted down-regulation of transcripts associated with oxidative pathways in cardiac muscle of ATGL$^{-/-}$ mice

Notably, the tissue in which ATGL ablation modulated the largest number of biological processes was CM (Fig. 3). A total of 419 genes

ATGL-/- WAT (257/54)										
ATGL-/- BAT (1329/538)	34									
ATGL-/- CM (1594/419)	40	318								
ATGL-/- LIV (433/144)	16	50	69							
ATGL-/- SM (390/72)	3	41	46	5						
HSL-/- WAT (915/197)	35	110	77	18	21					
HSL-/- BAT (877/182)	11	79	100	15	80	143				
HSL-/- CM (192/12)	2	15	16	4	1	10	6			
HSL-/- LIV (211/41)	2	11	12	9	4	31	12	0		
HSL-/- SM (1357/276)	6	39	20	11	47	192	113	8	20	
	ATGL-/- WAT (257/54)	ATGL-/- BAT (1329/538)	ATGL-/- CM (1594/419)	ATGL-/- LIV (433/144)	ATGL-/- SM (390/72)	HSL-/- WAT (915/197)	HSL-/- BAT (877/182)	HSL-/- CM (192/12)	HSL-/- LIV (211/41)	HSL-/- SM (1357/276)

Fig. 2. Number of commonly up- or down-regulated ESTs comparing two tissues of ATGL$^{-/-}$ and HSL$^{-/-}$ mice. First number in parentheses corresponds to the number of ESTs differentially expressed in that tissue. Second number in parentheses corresponds to the number of ESTs differentially expressed in that tissue with no missing value in all other tissues.

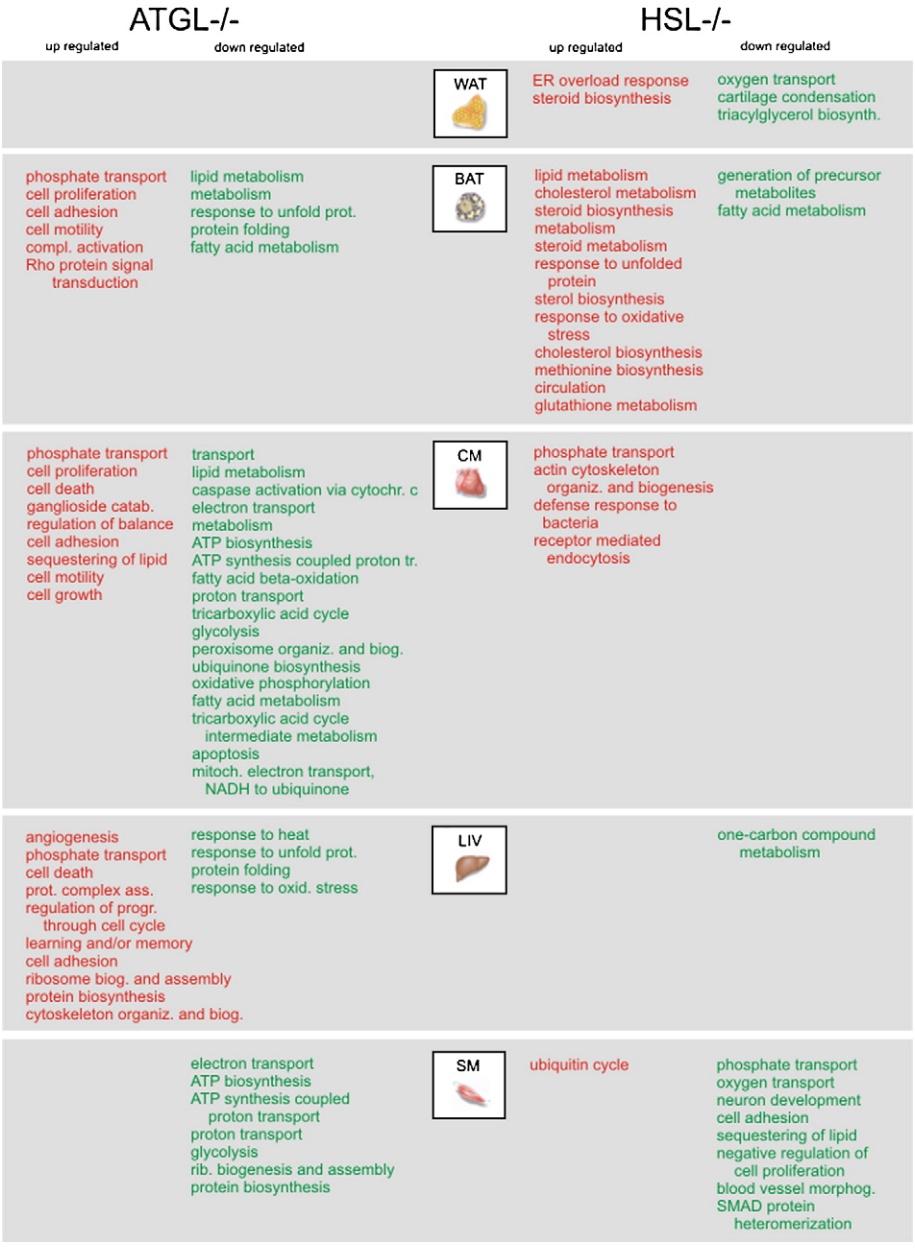

Fig. 3. Significantly overrepresented Gene Ontology terms (GO category "biological process") for up- and down-regulated genes in all analyzed tissues for both ATGL$^{-/-}$ and HSL$^{-/-}$ mice.

were found to be differentially expressed in this tissue. In marked contrast, only 12 genes were deregulated in HSL$^{-/-}$ CM. Most of the modulated genes in CM of ATGL$^{-/-}$ mice were assigned to catabolic and oxidative pathways, including the tricarboxylic acid cycle, lipid metabolism, fatty acid β-oxidation, glycolysis, electron transport, oxidative phosphorylation, and ATP biosynthesis.

The down-regulated genes included mediators of glucose metabolism such as the glucose transporters *Slc2a4* and *Slc2a3* and key glycolytic enzymes, i.e., pyruvate dehydrogenase (*Pdha1, Pdhb*) and phosphofructokinase (*Pfkm*). Differentially expressed genes involved in lipid metabolism included genes for fatty acid uptake (solute carrier family 27 (fatty acid transporter) (*Slc27a1*) and fatty acid oxidation (acetyl-coenzyme A dehydrogenase) (*Acadl*)), the mitochondrial carnitine palmitoyltransferase transporters (*Cpt1b, Cpt2*), and carnitine acetyltransferase (*Crat*). Genes of the tricarboxylic acid cycle that were down-regulated included succinate dehydrogenase (*Sdhd*), isocitrate dehydrogenase 2 (NADP$^+$) (*Idh2*), fumarate hydratase 1 (*Fh1*), and malate dehydrogenase 1 and 2 (*Mdh1, Mdh2*).

Taken together, these results suggest that ablation of ATGL, but not of HSL, in CM results in a concerted down-regulation of the oxidative pathways required for energy production from alternative substrates such as glucose and fatty acids. The genes observed to be differentially expressed in ATGL$^{-/-}$ mice are unaffected in HSL$^{-/-}$ mice (e.g., *Fh1, Idh2*) or else the effects were undetectable.

Fatty acid β-oxidation is down-regulated in both ATGL$^{-/-}$ and HSL$^{-/-}$ BAT

The largest number of differentially expressed genes were detected in BAT—a total of 720 (see Fig. 1: 538 differentially expressed ESTs in ATGL$^{-/-}$ and 182 in HSL$^{-/-}$). Notably, analysis of the deregulated genes in ATGL$^{-/-}$ BAT revealed a significant down-regulation of lipid and fatty acid metabolism in this tissue (Fig. 3). The cellular localizations of the gene products deregulated in ATGL$^{-/-}$ BAT are shown in Fig. 4 and [14]. The down-regulated genes associated with fatty acid oxidation include acyl-coenzyme A dehydrogenase very long chain (*Acadvl*), involved in the first step of fatty acid β-oxidation; dodecenoyl-

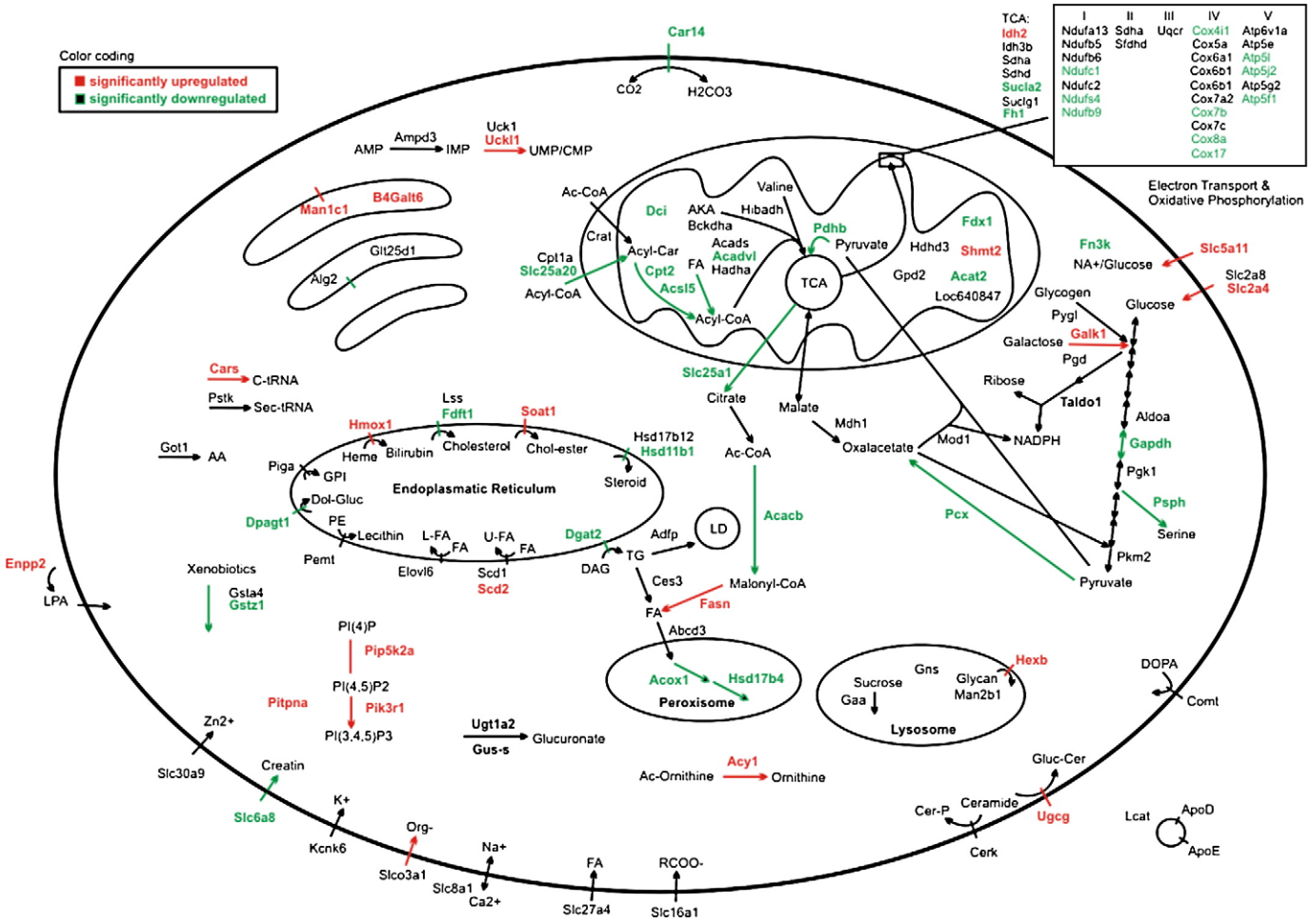

Fig. 4. Cellular role and localization of differentially expressed genes in BAT of ATGL$^{-/-}$ mice.

coenzyme A δ-isomerase (3,2 *trans*-enoyl-coenyme A isomerase) (*Dci*), responsible for isomerization of auxiliary steps for mitochondrial β-oxidation; carnitine palmitoyltransferase 2 (*Cpt2*), which facilitates the binding of coenzyme A to long-chain fatty acids for mitochondrial β-oxidation; acyl-CoA synthetase long-chain family member 5 (*Acsl5*), involved in activation of long-chain fatty acids for both the synthesis of cellular lipids and their degradation via β-oxidation; and hydroxysteroid dehydrogenase (*Hsd17b4*) and acyl-coenzyme A oxidase 1, palmitoyl (*Acox1*), enzymes of the peroxisomal β-oxidation pathway (Fig. 4). Remarkably, many genes encoding enzymes of the tricarboxylic acid cycle, for instance, fumarate hydratase 1 (*Fh1*) and succinate-coenzyme A ligase (*Sucla2*), were also down-regulated, as were genes encoding members of the electron transport chain (Fig. 4).

Fatty acid metabolism was also down-regulated in HSL$^{-/-}$ mice, although to a smaller extent than in ATGL$^{-/-}$ mice. The following genes were down-regulated: one gene of the β-oxidation pathway (*Echs1*), one fatty acid transporter (*Slc27a1*), the lipoprotein lipase (*Lpl*), the uncoupling protein 3 (*Ucp3*), and ankyrin repeat domain 23 (*Ankrd23*). The latter gene encodes a protein whose physiological function is not clear [15] but which is putatively involved in lipid metabolism.

Expression changes underlying the use of an alternative energy source in SM of HSL$^{-/-}$ mice

The observed changes in gene expression in HSL$^{-/-}$ mice were most pronounced in SM. Furthermore, the number of deregulated ESTs in HSL$^{-/-}$ SM was significantly greater than in ATGL$^{-/-}$ SM (276 in HSL$^{-/-}$ and 72 in ATGL$^{-/-}$ mice). Fig. 5 and [14] show the cellular localization of the deregulated genes involved in metabolism in SM of HSL$^{-/-}$ mice. Among these, genes involved in lipid uptake (*Lpl*), lipid synthesis (the fatty acid synthase, *Fasn*), and lipid storage (the adipose differentiation-related protein, *Adfp*) were down-regulated. At the same time, genes involved in glycogen and glucose utilization were up-regulated, for instance, the glucose transporters *Slc2a3* and *Slc2a4,* the glycolytic enzyme enolase 2 (*Eno2*), amylo-1,6-glucosidase, 4-α-glucanotransferase (*Agl*), and several genes encoding components of the electron transport chain. Taken together, these changes are consistent with previous studies suggesting a metabolic switch from lipid to carbohydrate metabolism in SM in HSL$^{-/-}$ mice [16].

Correspondence between gene expression and phenotype

Our comparative transcriptomic analysis of lipase-deficient metabolic tissues provided a bird's eye view of molecular processes at the organism level and enabled us to correlate changes in gene expression with the corresponding phenotypes (Table 1). Specifically, defective cold adaptation and lipid accumulation in the heart of the ATGL$^{-/-}$ mouse were mirrored by changes in the levels of transcripts associated with the corresponding biological processes. Moreover, our results shed new light on the observed cardiac insufficiency of ATGL$^{-/-}$ mice: energy starvation in CM.

Deficient thermogenesis in ATGL$^{-/-}$ mice

We have demonstrated that genes involved in lipid metabolism and fatty acid β-oxidation are down-regulated in ATGL$^{-/-}$ BAT. This is consistent with current theories that place ATGL as the first enzyme in

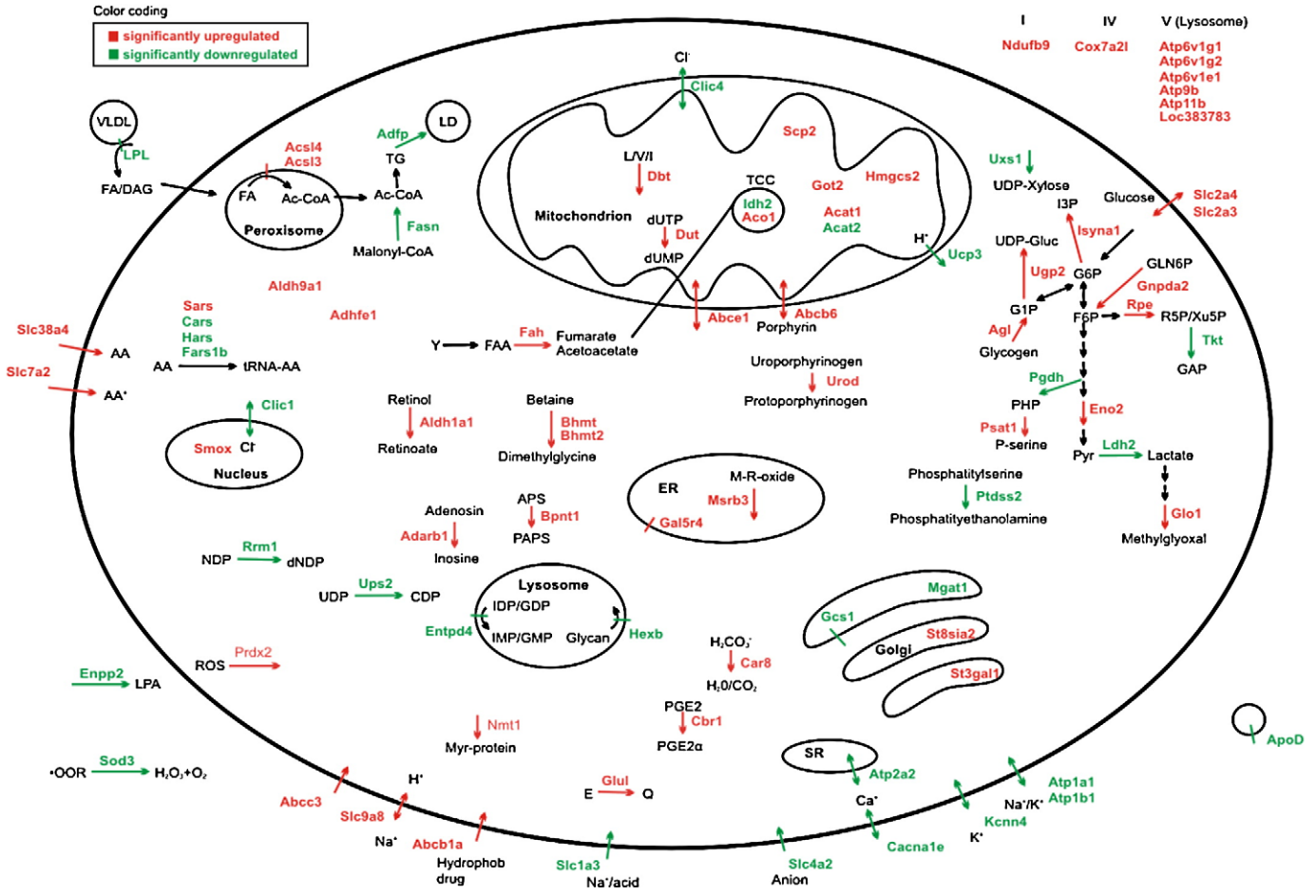

Fig. 5. Cellular role and localization of differentially expressed genes in SM of HSL$^{-/-}$ mice.

the TG hydrolytic chain, with HSL acting subsequently on DG. Thus, a lack of ATGL would lead to a net reduction in fatty acids to be metabolized and thus a reduced requirement for β-oxidation. We also observed the down-regulation of genes involved in the tricarboxylic acid cycle and in electron transport (Fig. 4). Taken together, these results suggest that ATGL deficiency results in a general impairment of energy production pathways in BAT. Consistent with this, ATGL$^{-/-}$ mice exhibit reduced oxygen consumption and severe defects in thermoregulation, i.e., they are cold sensitive [12].

Lipid accumulation in CM of ATGL$^{-/-}$ mice

Our analysis of CM in ATGL$^{-/-}$ mice revealed the down-regulation of the transcripts of genes involved in fatty acid uptake and in β-oxidation, such as the fatty acid transporter *Slc27a1* and the mitochondrial fatty acid transporters *Cpt1b* and *Cpt2*. This suggests that TG accumulation resulting from the impairment of lipid hydrolysis subsequently induces a negative feedback regulation that decreases fatty acid influx and oxidation.

Energy starvation in CM of ATGL$^{-/-}$ mice

The results of this study reveal concerted down-regulation of oxidative pathways in CM in the ATGL-deficient mouse model. Under physiological conditions, CM is able to switch over to the use of glucose as an energy source. As shown in Fig. 3, both glycolysis and the tricarboxylic acid cycle were down-regulated in ATGL$^{-/-}$ CM. Furthermore, the glucose transporters *Slc2a3* and *Slc2a4* were also down-regulated. Our results therefore do not suggest a metabolic switch to glucose utilization as under physiological conditions. The consequence of the concerted down-regulation of oxidative processes is energy starvation in CM and consequent cardiac insufficiency.

Toxicity of lipid intermediates of ATGL$^{-/-}$ mice

TGs cannot be hydrolyzed in ATGL$^{-/-}$ mice and thus accumulate, resulting in the down-regulation of a range of metabolic processes in metabolic tissues. Lipid accumulation can furthermore lead to adverse effects on other processes. Processes that were up-regulated in the ATGL$^{-/-}$ mouse include cell death in cardiac muscle and in liver, in

Table 1
Phenotypic characteristics of the lipase-deficient mouse models (Refs. [12] and [4])

	ATGL$^{-/-}$	HSL$^{-/-}$
Obesity	Mild	No
TG in heart	Yes	No
Defective thermoregulation	Yes	No
Fat cell hypertrophy	Yes	Yes
β-Adrenergic-stimulated lipolysis in WAT	No	No
Plasma FFA (fed/fasted)	Reduced/reduced	Reduced
Plasma TG (fed/fasted)	Equal/reduced	Equal/reduced
Plasma hydroxybutyrate (fed/fasted)	Equal/reduced	Equal/reduced
Plasma total cholesterol (fed/fasted)	Equal/reduced	Equal/reduced
Plasma HDL-cholesterol (fasted)	Reduced	Increased
Plasma insulin	Reduced/equal	
Plasma glucose (fed/fasted)	Equal/equal	/equal
RQ fasting	Increased	Equal
Oxygen consumption fasting	Reduced	Equal

accordance with the concept of lipotoxicity [17], in which lipid species exhibit adverse effects in nonadipose tissues.

Discussion

In this study, we performed the first genome-wide examination of the modulation of biological processes in response to genetic ablation of two intracellular lipases, ATGL and HSL. Our chosen approach was to profile gene expression in the metabolic tissues of ATGL- and the HSL-deficient mice using DNA microarrays. This comparative transcriptomics approach and subsequent comprehensive bioinformatics analyses suggest several important conclusions.

First, the transcript signatures of the metabolic tissues of the two mouse models were distinct and tissue specific. Strikingly, very few genes were deregulated in both models. At the level of biological processes, only fatty acid metabolism in BAT was modulated in the same manner in both ATGL$^{-/-}$ and HSL$^{-/-}$ mice. That said, the deregulated genes underlying this change were different in the two mouse models. The most pronounced modulation of biological processes was observed in CM of the ATGL$^{-/-}$ mouse and in SM of the HSL$^{-/-}$ mouse. Interestingly, only moderate changes in the levels of transcripts associated with identifiable biological processes were observed in WAT. In wild-type mice, both lipases are highly expressed in this tissue.

Second, the transcript signatures provided novel insights into the metabolic derangements characteristic of ATGL$^{-/-}$ mice. ATGL$^{-/-}$ mice have massive TG accumulation in heart tissue, which leads to cardiac insufficiency and premature death [12]. In the heart, dietary fatty acids are directed either to oxidation or to TG depots. Previous studies had already suggested a tight regulation of fatty acid uptake, oxidation, and lipid storage and it is thought that an imbalance between fatty acid influx and oxidation causes cardiac lipid droplet formation [18,19]. Our results in ATGL$^{-/-}$ mice lend support to the hypothesis that these processes are regulated in a concerted manner, since lack of intracellular TG mobilization also impairs fatty acid influx and oxidation, as demonstrated by the strong down-regulation of genes involved in fatty acid uptake, β-oxidation and TG synthesis. The biochemical consequences of these down-regulations have been previously shown [12]. Another interesting finding was the down-regulation of the pathways for glucose utilization, suggesting energy starvation in CM of ATGL$^{-/-}$ mice.

Third, the data provide evidence for a high degree of interconnectivity of metabolic networks and other biological processes. This has important implications for the development of drugs that modulate the activity of rate-limiting enzymes in lipid metabolism (despite intensive efforts in preclinical and clinical research, very few approved drugs target such key enzymes). Because metabolic networks are so highly interconnected, perturbation at one key point can have profound and unpredictable effects on many other metabolic pathways. Metabolic pathways are strongly evolutionarily conserved as recently demonstrated by the identification of an ATGL homolog in yeast [20]. Moreover, these pathways are controlled through hard-wired neural, metabolic, and hormonal signals. Evidence that metabolic intermediates are signaling molecules for a variety of biological processes including cell death, cell proliferation, and apoptosis must also be taken into account in the drug development process. The modulating effects of the signaling molecules can be direct or indirect and further studies in which lipid species are measured will be necessary to identify the key ligands and their target molecules. Thus, drug development for treatment of obesity will be successful only if large-scale technologies, including microarrays and metabolomics techniques, are used to elucidate the cellular changes in the relevant tissues.

Conclusion

This study is the first to demonstrate the specific effects of genetic ablation of the intracellular lipases ATGL and HSL on the mouse transcriptome in metabolic tissues. Our findings show largely distinct tissue-specific modulation of biological processes in ATGL$^{-/-}$ and HSL$^{-/-}$ mice. The transcript signatures observed also provided novel insights into the metabolic derangements characteristic of ATGL$^{-/-}$ mice. The specific alterations observed in this work expand the understanding of the toxicological consequences of lipase inhibition and highlight metabolic and signaling pathways previously not known to be affected by intracellular lipases.

Materials and methods

Animal procedures. ATGL$^{-/-}$ [12] and HSL$^{-/-}$ [4] mice and their respective wild-type littermates were used for this study. Animals were kept on a chow diet (4.5% w/w fat) and on a 12-h light/dark cycle. Tissues were collected only from male mice in a fed state (ATGL$^{-/-}$ at the age of 3 months, HSL$^{-/-}$ at the age of 6 months). All animal procedures used were approved by the Austrian Bundesministerium für Bildung, Wissenschaft, und Kultur.

Sample preparation. Five different tissues—WAT, BAT, CM, LIV, and SM—were isolated (six mice per tissue). RNA from these tissues was extracted with the TRIzol reagent (Invitrogen) according to the manufacturer's protocol. For each tissue, total RNA was pooled from two mice and experiments were performed in triplicate.

Gene expression and data analysis. The mouse cDNA microarrays and the hybridization protocols used have been described previously [21]. Briefly, the spotted microarrays contain >27,000 elements with mouse cDNA clones representing 16,000 different genes (UniGene clusters). Twenty micrograms of total RNA from each tissue of interest from ATGL$^{-/-}$ (HSL$^{-/-}$) mice and ATGL$^{+/+}$ (HSL$^{+/+}$) mice was reverse transcribed into cDNA, which was then indirectly labeled with Cy5 or Cy3, respectively. To account for technical variation, procedures were repeated using the same samples with reversed dye assignment. The microarrays were prehybridized with 5× SSC, 0.1% SDS, 1% BSA. Pairwise-labeled cDNA samples were combined and 20 μg of mouse Cot1 DNA and 20 μg of poly(A) DNA were added. The mixture was hybridized onto the slides overnight at 42 °C. Following washing, slides were scanned with a GenePix 4000B microarray scanner (Axon Instruments) at 10 μm resolution. The resulting TIFF images were analyzed with GenePix Pro 4.1 software (Axon Instruments). Features were filtered for low-quality spots. To obtain expression values for saturated spots, slides were scanned a second time with lower photomultiplier tube settings and reanalyzed [22]. Following subtraction of the local background, the arrays were global median and dye-swap normalized using ArrayNorm [23] and the resulting ratios $\log_2$ transformed. All experimental parameters, images, raw data, and transformed data were uploaded to the microarray database MARS [24] and submitted via MAGE-ML export to a public repository (ArrayExpress [25], Accession Nos. E-MARS-8, E-MARS-9, and A-MARS-5). After outliers were removed the median expression values of replicated ESTs on the microarray were calculated. Only ESTs with $z>1.5$ and significant replication ($p<0.05$) using the z test and assuming a standard normal distribution were considered differentially expressed and used for further analysis [26,27]. Expression values and z scores for differentially expressed ESTs were averaged over biological replicates. All calculations were implemented in PERL 5.8.0, and cluster analyses and visualizations were performed using Genesis [28].

Functional annotation, cellular role, and pathway context. For each of the selected EST sequences, we attempted to find the corresponding protein sequence as described previously [21]. All protein sequences were annotated de novo with >40 academic prediction tools that are integrated into the Annotator, a novel protein sequence analysis system [29]. Further information was retrieved from the Mouse Genome Informatics [30] and Entrez Gene [31] databases. Gene products were mapped onto known pathways and assigned putative cellular roles and subcellular localizations using a combination of PathwayExplorer [32], a literature survey, and domain-based assignments. Differentially expressed genes were also classified according to GO [13]. Significant GO terms for biological process, cellular component, and molecular function for proteins encoded by differentially expressed genes were identified by comparison with the GO assignment of all mouse proteins included in the RefSeq database [33] using the one-sided Fisher exact test. To account for multiple testing, p values were adjusted controlling for the false discovery rate (FDR) as proposed by Benjamini and Hochberg [34], and directed acyclic graphs for statistically overrepresented GO terms within the category "biological process" were constructed. Only terms with three or more entries from the dataset and with FDR <5% were considered statistically significant.

Validation of microarray data using real-time PCR. Microarray results were verified by quantitative real-time PCR for *Cpt2, Slc2a4, Ucp2, Dgat2, Mdh1, Mgll, G0s2, Klf4, Igf1,* and *Igfbp4* (sequences of primer pairs can be found in Supplementary File 2). The RNA samples from three biological replicates from wild-type and knockout mice (ATGL$^{-/-}$ and HSL$^{-/-}$) previously used for microarrays were used for qPCR. cDNA from 2.5 μg RNA was generated using Stratascript reverse transcriptase (Stratagene) according to the manufacturer's instructions. The reverse-transcription product was diluted in water and a volume corresponding to 20 ng original RNA used for qPCR. Quantitative real-time PCR amplification and detection were performed using the Sybr Green Master Mix (Applied Biosystems, Warrington, UK) in a fluorescence thermal cycler (ABI Prism 7000 sequence detection system; Applied Biosystems) according to the manufacturer's protocol. Each sample was quantified in duplicate. Gene expression was normalized using *Gtf2b* as a reference gene. Relative mRNA expression levels were calculated following the $\Delta\Delta C_t$

method. The $\Delta\Delta C_t$ values for each biological replicate were averaged and transformed to $\log_2$ ratios. A high degree of correlation between microarray data and real-time PCR data was found (r^2=0.86, Supplementary File 4).

Acknowledgments

This study was supported by the Austrian Ministry of Science and Research (GEN-AU Genome Program, Projects GOLD II and BIN II) and the Austrian Science Fund (Project SFB Lipotoxicity). M. Pinent is the recipient of a fellowship from the Generalitat de Catalunya, Spain. We are grateful to Dr. C. Wrighton for help with the preparation of the manuscript.

Appendix A. Supplementary data

Supplementary data associated with this article can be found, in the online version, at doi:10.1016/j.ygeno.2008.03.010.

References

[1] B.M. Spiegelman, J.S. Flier, Obesity and the regulation of energy balance, Cell 104 (2001) 531–543.
[2] P. Trayhurn, The biology of obesity, Proc. Nutr. Soc. 64 (2005) 31–38.
[3] C. Holm, Molecular mechanisms regulating hormone-sensitive lipase and lipolysis, Biochem. Soc. Trans. 31 (2003) 1120–1124.
[4] G. Haemmerle, R. Zimmermann, J.G. Strauss, D. Kratky, M. Riederer, G. Knipping, R. Zechner, Hormone-sensitive lipase deficiency in mice changes the plasma lipid profile by affecting the tissue-specific expression pattern of lipoprotein lipase in adipose tissue and muscle, J. Biol. Chem. 277 (2002) 12946–12952.
[5] J.i. Osuga, S. Ishibashi, T. Oka, H. Yagyu, R. Tozawa, A. Fujimoto, F. Shionoiri, N. Yahagi, F.B. Kraemer, O. Tsutsumi, N. Yamada, Targeted disruption of hormone-sensitive lipase results in male sterility and adipocyte hypertrophy, but not in obesity, Proc. Natl. Acad. Sci. U. S. A. 97 (2000) 787–792.
[6] S.P. Wang, N. Laurin, J. Himms-Hagen, M.A. Rudnicki, E. Levy, M.F. Robert, L. Pan, L. Oligny, G.A. Mitchell, The adipose tissue phenotype of hormone-sensitive lipase deficiency in mice, Obes. Res. 9 (2001) 119–128.
[7] K. Harada, W.J. Shen, S. Patel, V. Natu, J. Wang, J. Osuga, S. Ishibashi, F.B. Kraemer, Resistance to high-fat diet-induced obesity and altered expression of adipose-specific genes in HSL-deficient mice, Am. J. Physiol. Endocrinol. Metab. 285 (2003) E1182–E1195.
[8] C.M. Jenkins, D.J. Mancuso, W. Yan, H.F. Sims, B. Gibson, R.W. Gross, Identification, cloning, expression, and purification of three novel human calcium-independent phospholipase A2 family members possessing triacylglycerol lipase and acylglycerol transacylase activities, J. Biol. Chem. 279 (2004) 48968–48975.
[9] J.A. Villena, S. Roy, E. Sarkadi-Nagy, K.H. Kim, H.S. Sul, Desnutrin, an adipocyte gene encoding a novel patatin domain-containing protein, is induced by fasting and glucocorticoids: ectopic expression of desnutrin increases triglyceride hydrolysis, J. Biol. Chem. 279 (2004) 47066–47075.
[10] R. Zimmermann, J.G. Strauss, G. Haemmerle, G. Schoiswohl, R. Birner-Gruenberger, M. Riederer, A. Lass, G. Neuberger, F. Eisenhaber, A. Hermetter, R. Zechner, Fat mobilization in adipose tissue is promoted by adipose triglyceride lipase, Science 306 (2004) 1383–1386.
[11] E. Smirnova, E.B. Goldberg, K.S. Makarova, L. Lin, W.J. Brown, C.L. Jackson, ATGL has a key role in lipid droplet/adiposome degradation in mammalian cells, EMBO Rep. 7 (2006) 106–113.
[12] G. Haemmerle, A. Lass, R. Zimmermann, G. Gorkiewicz, C. Meyer, J. Rozman, G. Heldmaier, R. Maier, C. Theussl, S. Eder, D. Kratky, E.F. Wagner, M. Klingenspor, G. Hoefler, R. Zechner, Defective lipolysis and altered energy metabolism in mice lacking adipose triglyceride lipase, Science 312 (2006) 734–737.
[13] M.A. Harris, J. Clark, A. Ireland, J. Lomax, M. Ashburner, R. Foulger, K. Eilbeck, S. Lewis, B. Marshall, C. Mungall, J. Richter, G.M. Rubin, J.A. Blake, C. Bult, M. Dolan, H. Drabkin, J.T. Eppig, D.P. Hill, L. Ni, M. Ringwald, et al., The Gene Ontology (GO) database and informatics resource, Nucleic Acids Res. 32 (2004) D258–D261.
[14] Differential transcriptional modulation of biological processes in adipocyte triglyceride lipase and hormone sensitive lipase deficient mice. [http://genome.tugraz.at/ATGL-HSL/] (2008).
[15] K. Ikeda, N. Emoto, M. Matsuo, M. Yokoyama, Molecular identification and characterization of a novel nuclear protein whose expression is up-regulated in insulin-resistant animals, J. Biol. Chem. 278 (2003) 3514–3520.
[16] O. Hansson, M. Donsmark, C. Ling, P. Nevsten, M. Danfelter, J.L. Andersen, H. Galbo, C. Holm, Transcriptome and proteome analysis of soleus muscle of hormone-sensitive lipase-null mice, J. Lipid Res. 46 (2005) 2614–2623.
[17] J.E. Schaffer, Lipotoxicity: when tissues overeat, Curr. Opin. Lipidol. 14 (2003) 281–287.
[18] J. Suzuki, W.J. Shen, B.D. Nelson, S.P. Selwood, G.M. Murphy Jr., H. Kanehara, S. Takahashi, K. Oida, I. Miyamori, F.B. Kraemer, Cardiac gene expression profile and lipid accumulation in response to starvation, Am. J. Physiol. Endocrinol. Metab. 283 (2002) E94–E102.
[19] J. Suzuki, W.J. Shen, B.D. Nelson, S. Patel, J.H. Veerkamp, S.P. Selwood, G.M. Murphy Jr., E. Reaven, F.B. Kraemer, Absence of cardiac lipid accumulation in transgenic mice with heart-specific HSL overexpression, Am. J. Physiol. Endocrinol. Metab. 281 (2001) E857–E866.
[20] C.F. Kurat, K. Natter, J. Petschnigg, H. Wolinski, K. Scheuringer, H. Scholz, R. Zimmermann, R. Leber, R. Zechner, S.D. Kohlwein, Obese yeast: triglyceride lipolysis is functionally conserved from mammals to yeast, J. Biol. Chem. 281 (2006) 491–500.
[21] H. Hackl, T.R. Burkard, A. Sturn, R. Rubio, A. Schleiffer, S. Tian, J. Quackenbush, F. Eisenhaber, Z. Trajanoski, Molecular processes during fat cell development revealed by gene expression profiling and functional annotation, Genome Biol. 6 (2005) R108.
[22] H. Lyng, A. Badiee, D.H. Svendsrud, E. Hovig, O. Myklebost, T. Stokke, Profound influence of microarray scanner characteristics on gene expression ratios: analysis and procedure for correction, BMC Genomics 5 (2004) 10.
[23] R. Pieler, F. Sanchez-Cabo, H. Hackl, G.G. Thallinger, Z. Trajanoski, ArrayNorm: comprehensive normalization and analysis of microarray data, Bioinformatics 20 (2004) 1971–1973.
[24] M. Maurer, R. Molidor, A. Sturn, J. Hartler, H. Hackl, G. Stocker, A. Prokesch, M. Scheideler, Z. Trajanoski, MAR: Smicroarray analysis, retrieval, and storage system, BMC Bioinformatics 6 (2005) 101.
[25] A. Brazma, H. Parkinson, U. Sarkans, M. Shojatalab, J. Vilo, N. Abeygunawardena, E. Holloway, M. Kapushesky, P. Kemmeren, G.G. Lara, A. Oezcimen, P. Rocca-Serra, S.A. Sansone, ArrayExpress—a public repository for microarray gene expression data at the EBI, Nucleic Acids Res. 31 (2003) 68–71.
[26] C. Cheadle, M.P. Vawter, W.J. Freed, K.G. Becker, Analysis of microarray data using Z score transformation, J. Mol. Diagn. 5 (2003) 73–81.
[27] C.D. Toscano, V.V. Prabhu, R. Langenbach, K.G. Becker, F. Bosetti, Differential gene expression patterns in cyclooxygenase-1 and cyclooxygenase-2 deficient mouse brain, Genome Biol. 8 (2007) R14.
[28] A. Sturn, J. Quackenbush, Z. Trajanoski, Genesis: cluster analysis of microarray data, Bioinformatics 18 (2002) 207–208.
[29] Wildpaner M. et al., Annotator: Large Scale Sequence Annotation System. Available online at http://annotator.imp.univie.ac.at/.
[30] J.A. Blake, J.E. Richardson, C.J. Bult, J.A. Kadin, J.T. Eppig, MGD: the Mouse Genome Database, Nucleic Acids Res. 31 (2003) 193–195.
[31] D. Maglott, J. Ostell, K.D. Pruitt, T. Tatusova, Entrez Gene: gene-centered information at NCBI, Nucleic Acids Res. 33 (2005) database issue:D54-D58.
[32] B. Mlecnik, M. Scheideler, H. Hackl, J. Hartler, F. Sanchez-Cabo, Z. Trajanoski, PathwayExplorer: web service for visualizing high-throughput expression data on biological pathways, Nucleic Acids Res. 33 (2005) W633–W637.
[33] K.D. Pruitt, T. Tatusova, D.R. Maglott, NCBI reference sequences (RefSeq): a curated non-redundant sequence database of genomes, transcripts and proteins, Nucleic Acids Res. 35 (2007) D:61–D:65.
[34] Y. Benjamini, Y. Hochberg, Controlling the false discovery rate—a practical and powerful approach to multiple testing, J. R. Stat. Soc. Ser. B Method. 57 (1995) 289–300.